

## Letter

## Indium tin oxide-free semi-transparent inverted polymer solar cells using conducting polymer as both bottom and top electrodes

Steven K. Hau<sup>a</sup>, Hin-Lap Yip<sup>a,b</sup>, Jingyu Zou<sup>a</sup>, Alex K.-Y. Jen<sup>a,b,\*</sup><sup>a</sup> Department of Materials Science and Engineering, Institute of Advanced Materials and Technology, University of Washington, Seattle, Washington 98195-2120, United States<sup>b</sup> Institute of Advanced Materials and Technology, University of Washington, Seattle, Washington 98195-2120, United States

## ARTICLE INFO

## Article history:

Received 20 May 2009

Received in revised form 25 June 2009

Accepted 26 June 2009

Available online 3 July 2009

## Keywords:

Inverted solar cell

Semi-transparent

PEDOT: PSS

ITO replacement

## ABSTRACT

Poly(3,4-ethylenedioxythiophene):poly(styrenesulfonate) (PEDOT:PSS) is investigated as a transparent cathode to replace indium tin oxide (ITO) in inverted polymer solar cells. Increasing the thickness of the PEDOT:PSS electrode leads to a reduction in transparency and sheet resistance which lowers the photocurrent but increases the fill factor of the solar cells. The offset of photocurrent and fill factor as the thickness is increased leads to a saturation of the power conversion efficiency to ~3%. These electrodes were applied to flexible substrates showing similar device performance to glass based devices. Cyclic bending test of these flexible polymer electrodes show improved conversion efficiency retention (~92%) when compared to flexible ITO based electrodes (~50%) after 300 bend cycles. In addition to using PEDOT:PSS as a cathode replacement for ITO in inverted solar cells, its use as a semi-transparent anode replacement to Ag is also examined. Semi-transparent inverted solar cells fabricated with ITO as the cathode and PEDOT:PSS as the top anode electrode were demonstrated showing efficiencies of ~2.51% while replacement of both ITO and Ag with PEDOT:PSS as both the cathode and anode show efficiencies of ~0.47%.

© 2009 Elsevier B.V. All rights reserved.

Organic polymer-based solar cells (OSCs) promise a low-cost renewable energy solution to the current energy crisis due to its potential to be fabricated onto large areas by simple roll-to-roll printing and coating technologies. OSCs based on semiconducting polymer/fullerene bulk-heterojunction blends consisting of interpenetrating networks of electron-donor and -acceptor materials have lead to conversion efficiencies of ~4–5% [1,2]. However, these devices utilize indium tin oxide (ITO) as the hole collecting transparent conducting anode and a low work function metal as the electron collecting cathode. ITO is typically processed at high temperatures to improve crystallinity and conductivity which can only be done on rigid

substrates such as glass. Lower conductivity ITO can be processed onto flexible plastic substrates, but under numerous bending cycles, formation and propagation of cracks occur on the ITO which led to significant degradation of the conductivity and performance [3]. Additionally, the increasing costs of indium may prevent large scale usage of ITO as an electrode material for low-cost polymer-based solar cells. Other alternatives such as carbon nanotubes [4–6], graphene [7,8], metal grids/meshes [9–11], doped metal oxides [12,13] and organic polymers [3,14,15] to replace ITO as the transparent electrode have already been investigated. One particular organic based electrode material of interest is PEDOT:PSS due to its solution processibility which makes them compatible with the concept of large scale roll-to-roll processing. In addition, the mechanical properties of the organic polymer on plastic flexible substrates are much better than ITO. The typical formulation of PEDOT:PSS from Stark has low conductivity,

\* Corresponding author. Address: Department of Materials Science and Engineering, Institute of Advanced Materials and Technology, University of Washington, Seattle, Washington 98195-2120, United States.

E-mail address: [ajen@u.washington.edu](mailto:ajen@u.washington.edu) (A.K.-Y. Jen).

but has been found to improve by two to three orders (300–600 S/cm) by adding high boiling point polar compounds or solvents (diethylene glycol, ethylene glycol, dimethylsulfoxide, sorbitol, mannitol, glycerol) into the solution mixture. The exact reason for the improvement is still unclear, but has been suggested to be linked to changes in the PEDOT morphology and chain interaction [16].

There have been many demonstrations of utilizing PEDOT:PSS as a replacement to ITO as the transparent anode electrode in the conventional device architecture, however, these electrodes show a much lower conversion efficiency compared to ITO due to the lower conductivity of the PEDOT:PSS [17–19]. Recently, it was demonstrated by improving the PEDOT:PSS conductivity through processing with a high boiling point solvent, these organic polymer electrodes could reach efficiencies as high as 3% [3]. The top cathode electrode in these devices is still deposited by high vacuum which makes the processing less ideal for low-cost solar cells. To avoid using high vacuum to deposit the top electrode, an inverted architecture can be used which uses a high work function metal anode (Ag, Au) to collect holes and an metal oxide ( $\text{TiO}_2$ , ZnO) as an electron selective layer at the ITO interface to collect electrons. Previously, we have demonstrated that this type of unencapsulated inverted architecture solar cell using an evaporated Ag electrode stored 40 days in ambient retains over 80% of its conversion efficiency [20]. Furthermore, we demonstrated the possibility to utilize non-vacuum solution processible Ag nanoparticles as the top electrode in inverted solar cells by spraycoating leading to efficiencies as high as 3% [21]. It has already recently been demonstrated that PEDOT:PSS can also be used as the replacement anode electrode (energy level of  $-5.1$  eV) in inverted solar cells by spraycoating the polymer. However, due to the thick films formed from spraycoating, the electrodes are non-transparent and require high vacuum to remove excess moisture to improve the performance [22]. There have been currently no studies on utilizing PEDOT:PSS as a replacement cathode electrode to replace ITO as the transparent charge collecting contact in inverted solar cells.

This letter reports on the replacement of the ITO transparent conducting oxide electrode with a solution processible PEDOT:PSS electrode as the electron collecting cathode in inverted solar cells. The thickness of the PEDOT:PSS electrode was varied showing that the thickness can affect both the transparency and sheet resistance of the electrode

and therefore the final performance of the solar cell. These electrodes were also applied to flexible polymer substrates showing similar performance to glass substrates. These inverted flexible substrate PEDOT:PSS electrode devices show  $\sim 20\%$  lower in conversion efficiency compared to ITO based flexible substrate inverted devices. Cyclic bending tests were performed on these flexible substrates showing slight performance degradation from the PEDOT:PSS based electrodes while the ITO based electrodes show significant degradation after 300 bend cycles. PEDOT:PSS was also used to replace the anode Ag electrode in ITO based inverted solar cells demonstrating a semi-transparent solar cell. The semi-transparency of these cells allows for new potential power generating applications such as solar windows or other applications that require semi-transparency. Additionally, both the top anode and bottom cathode electrodes were replaced with PEDOT:PSS demonstrating a completely solution processed semi-transparent inverted solar cell.

The inverted device architectures that were used in this study are shown in Fig. 1. To fabricate the ITO electrode based inverted solar cells, ITO-coated glass substrates ( $15 \Omega/\square$ ) and ITO-coated plastic substrates ( $60 \Omega/\square$ ) (Bay-view Optics) were cleaned with detergent, de-ionized water, acetone, and isopropyl alcohol. A thin layer of ZnO nanoparticles (ZnO-NPs) ( $\sim 50$  nm), synthesized using the method described by Beek et al. [23], was spin-coated onto ITO-coated glass. A monolayer of  $\text{C}_{60}$ -SAM was then deposited as previously reported to improve the contact properties between the metal oxide and the active layer. [24,25]. Afterward, a chlorobenzene solution of poly(3-hexylthiophene) (P3HT) (Rieke Metals) and [6,6]-phenyl  $\text{C}_{61}$ -butyric acid methyl ester (PCBM) (American Dye Source) (60 mg/ml) with a weight ratio of (1:0.6) was spin-coated on the ZnO modified layer to achieve a thickness of ( $\sim 210$  nm) and annealed at  $160^\circ\text{C}$  for 10 min in an Ar filled glovebox. After annealing, PEDOT:PSS (CLEVIOS<sup>TM</sup> P VP Al 4083) was spin-coated onto the active layer to achieve a thickness of  $\sim 50$  nm and annealed for 10 min at  $120^\circ\text{C}$ . The silver electrode was vacuum deposited (100 nm) at a pressure of  $1 \times 10^{-6}$  torr to complete the device. For PEDOT:PSS electrode based inverted solar cells, glass and plastic substrates were cleaned with detergent, de-ionized water, acetone, and isopropyl alcohol. The substrates were treated by  $\text{O}_2$  plasma for 2 min to improve wettability of the PEDOT:PSS solution. A solution of PEDOT:PSS (CLEVIOS<sup>TM</sup> PH500) with the addition of 5% DMSO was sonicated

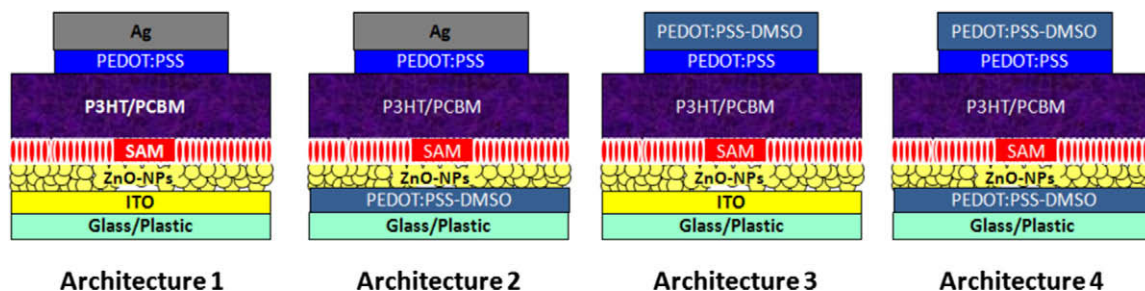
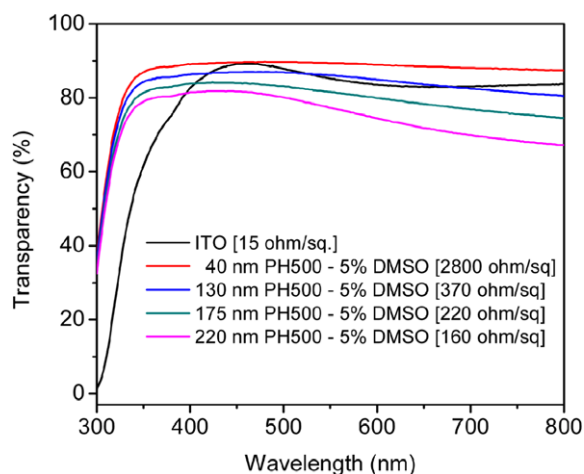
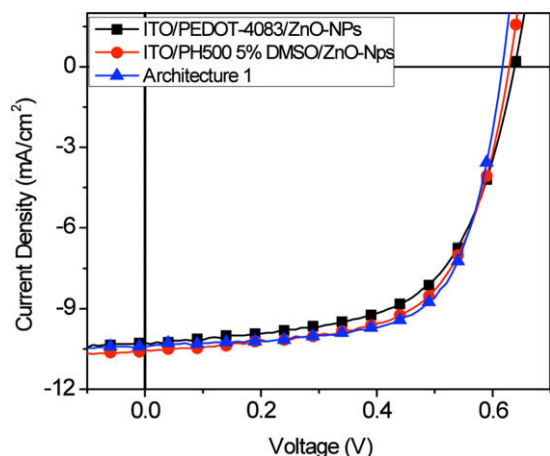


Fig. 1. Device architectures of the inverted solar cells using various cathode and anode electrodes.



**Fig. 2.** Transparency vs. wavelength of varying thicknesses of PEDOT:PSS - 5% DMSO electrodes on glass as compared to transparency of ITO on glass as referenced against air. Legend also indicates corresponding sheet resistances obtained as measured by 4-point probe.



**Fig. 3.** Illuminated  $J$ - $V$  characteristics of functioning inverted devices fabricated on ITO substrates with an  $\sim 80$  nm PEDOT:PSS CLEVIOS™ P VP Al 4083 or CLEVIOS™ PH500 with 5% DMSO inserted between the ITO and ZnO-NPs as compared to inverted devices with only ITO and ZnO-NPs.

for 5 min prior to use. For the first layer ( $\sim 40$  nm), the PEDOT:PSS solution was spin-coated onto the  $O_2$  plasma treated substrates at 7 krpm for 30 s and annealed at  $120^\circ\text{C}$  for a 2 min. Subsequent PEDOT:PSS layers were spin-coated at 2 krpm for 20 s and annealed at  $120^\circ\text{C}$  for a 2 min to achieve the desired thickness ( $\sim 130$  nm,  $\sim 175$  nm,  $\sim 220$  nm). The final PEDOT:PSS layers were annealed for 10 min at  $120^\circ\text{C}$  prior to depositing the rest of the layers as described in the ITO-based devices to complete the device. To deposit the top PEDOT:PSS anode electrodes for the semi-transparent devices, a patterned PDMS stamp was pressed onto the substrates of the top buffer PEDOT:PSS (CLEVIOS™ P VP Al 4083) and heated at  $120^\circ\text{C}$  for 30 s. After which, the sample was removed from the hotplate and the PDMS stamp was peeled off removing only the PEDOT:PSS from the active layer in contact with the stamp leaving behind a patterned PEDOT:PSS layer. Solutions of the PEDOT:PSS and DMSO were spin-coated at 3–5 krpm which coats only the area with the patterned PEDOT:PSS. Multiple PEDOT:PSS layers were built up by annealing the layers at  $120^\circ\text{C}$  for 2 min prior to spincoating the next layer. The unencapsulated solar cells were tested under ambient conditions using a Keithley 2400 SMU and an Oriel Xenon lamp (450 W) with an AM1.5 filter. A mask was used to define the device illumination area of  $0.0314\text{ cm}^2$  to minimize photocurrent generation from the edge of the electrodes [26,27]. The light intensity was calibrated to  $100\text{ mW/cm}^2$  using a calibrated silicon solar cell with a KG5 filter which has been previously standardized at the National Renewable Energy Laboratory.

To evaluate the possibility for using PEDOT:PSS as a transparent electrode to replace ITO, both the transparency and sheet resistance of different thicknesses of PEDOT:PSS processed with DMSO were measured. Fig. 2 shows the transparency as measured by UV-Vis spectroscopy of various thicknesses of PEDOT:PSS on glass substrates referenced against air which were compared to ITO-coated glass substrates. A PEDOT:PSS layer that is  $\sim 130$  nm thick has comparable transparency to the ITO-coated glass substrate. However, the sheet resistance of the PEDOT:PSS layer as measured by four point probe is  $\sim 25$  times higher than that of ITO ( $15\ \Omega/\square$ ). Thicker PEDOT:PSS layers show a reduction in sheet resistance to as low as  $160\ \Omega/\square$  with a

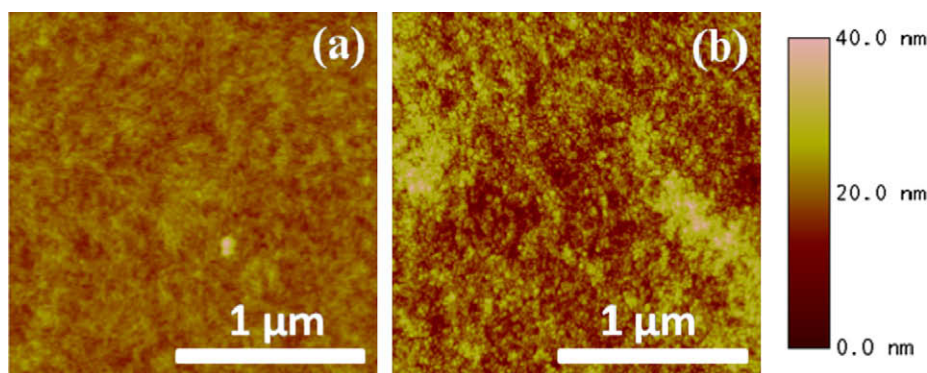


**Fig. 4.** (a) AFM image of  $\sim 130$  nm PEDOT:PSS - 5% DMSO layer coated onto glass. (b) AFM image of ZnO-NPs spin-coated on top of the PEDOT:PSS - 5% DMSO electrode.

~220 nm thick film, but also show a decrease in transparency due to the absorbance from the PEDOT:PSS film.

Replacement of ITO electrode with PEDOT:PSS as the anode has already been demonstrated in conventional architecture devices, but there has not been any study utilizing it as a cathode to collect electrons. To assess the feasibility of using PEDOT:PSS as a cathode, inverted solar cells were fabricated by spincoating a thick ~80 nm PEDOT:PSS layer from CLEVIOS™ P VP Al 4083 or CLEVIOS™ PH500 with 5% DMSO onto ITO-coated glass substrates prior to spincoating the ZnO-NPs electron selective layer followed by the rest of the device layers as described in the experimental section. Interestingly, the inverted solar cells with the PEDOT:PSS inserted between the ITO and ZnO-NPs layers behaved similarly to devices without the PEDOT:PSS layer as can be seen by Fig. 3. It has already been shown in literature that the interface contact between the heavily p-doped PEDOT:PSS and the unintentionally heavily n-doped ZnO in solar cells can be ohmic leading to minimal energy losses and minimal degradation of the voltage in the cell [28]. From this result and finding, “ITO-free” inverted solar cells using PEDOT:PSS as the cathode and ZnO-NPs as the electron selective layer were investigated. An atomic force microscopy image of a ~130 nm PEDOT:PSS film on glass in Fig. 4a shows a relatively smooth topography having a surface roughness of 1.7 nm RMS. Fig. 4b shows a much rougher surface topography (4.1 nm RMS) and different morphology after spincoating the ZnO-NPs on top of the PEDOT:PSS layer signifying that the ZnO-NPs layer is coated on top.

The illuminated  $J$ - $V$  characteristics of the inverted solar cell devices fabricated with different electrode PEDOT:PSS thicknesses as compared to ITO-based devices are shown in Fig. 5a and Table 1 summarizes these device performance parameters. Devices fabricated using a ~40 nm thick PEDOT:PSS as the electrode had a short circuit current ( $J_{sc}$ ), fill factor (FF), and power conversion efficiency (PCE) of 9.59 mA/cm<sup>2</sup>, 39.4%, and 2.32% respectively. Increasing the PEDOT:PSS electrode thickness to ~130 nm lead to an improvement in the overall PCE reaching ~3.08%, however a lowering of the  $J_{sc}$  to 9.41 mA/cm<sup>2</sup> while an increase in FF to 53.3% is observed. Electrodes using a ~175 nm PEDOT:PSS film show further decrease in  $J_{sc}$  to 8.57 mA/cm<sup>2</sup> while further increasing of FF to 57.2% leading to efficiencies of 2.99%. Increasing the PEDOT:PSS electrode thickness to ~220 nm again shows further lowering of  $J_{sc}$  (8.15 mA/cm<sup>2</sup>) and improved FF (60.0%) which gives a PCE of 2.98%. This trend of lower photocurrent and increasing fill factor as a function of increasing PEDOT:PSS electrode thickness can be correlated to the lower transparency and reduced sheet resistance with increasing layer thickness. The transparency and sheet resistance of the electrodes are important to consider as they can affect both the photocurrent and fill factor device parameters. The lower transparency leads to a reduction of the potential photons that are able to be absorbed by the active layer therefore leads to lower photocurrent densities. The reduction in sheet resistance minimizes the resistance losses in the solar cells and improves fill factor. With higher sheet resistance, the energy

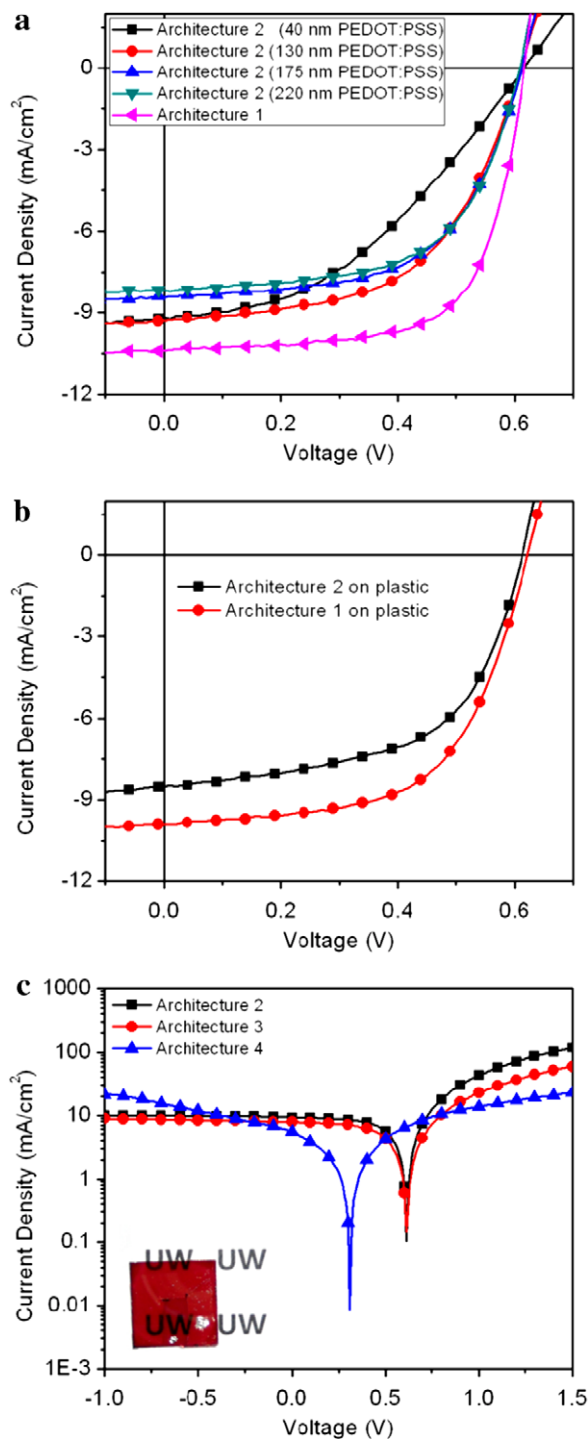


**Fig. 5.** (a) Illuminated  $J$ - $V$  characteristics of inverted devices fabricated from various thicknesses of PEDOT:PSS – 5% DMSO as cathode electrodes on glass as compared to ITO-based cathode electrodes. (b) Illuminated  $J$ - $V$  characteristics of inverted devices fabricated from PEDOT:PSS – 5% DMSO cathode electrodes on plastic substrates and ITO-based cathode electrodes on plastic substrates. (c) Illuminated log  $J$ - $V$  characteristics of inverted devices with architecture 2–4. Inset: semi-transparent solar cell using ITO cathode and PEDOT:PSS – 5% DMSO anode electrodes (architecture 3).



**Table 1**

Average device performance of inverted ZnO-NP/C<sub>60</sub>-SAM/P3HT:PCBM bulk-heterojunction solar cells fabricated using glass/PEDOT:PSS, plastic/PEDOT:PSS, glass/ITO and plastic/ITO as the cathode electrode and vacuum deposited Ag as the anode electrode. Average device performance of semi-transparent inverted solar cells using PEDOT:PSS as the anode electrode on glass/ITO and glass/PEDOT:PSS cathode electrodes. Average was obtained from multiple device tests.

Electrode (cathode)	Electrode (anode)	V <sub>oc</sub> (V)	J <sub>sc</sub> (mA/cm <sup>2</sup> )	FF (%)	PCE (%)
ITO/glass	Ag	0.62	10.25	66.6	4.20
PEDOT:PSS (~40 nm)/glass	Ag	0.61	9.59	39.4	2.32
PEDOT:PSS (~130 nm)/glass	Ag	0.61	9.41	53.3	3.08
PEDOT:PSS (~175 nm)/glass	Ag	0.61	8.57	57.2	2.99
PEDOT:PSS (~220 nm)/glass	Ag	0.61	8.15	60.0	2.98
ITO/plastic	Ag	0.61	9.86	61.2	3.73
PEDOT:PSS (~175 nm)/plastic	Ag	0.62	8.42	57.7	2.99
ITO/glass	PEDOT:PSS	0.61	7.86	52.0	2.51
PEDOT:PSS (~130 nm)/glass	PEDOT:PSS	0.31	5.49	27.7	0.47

lost from the lateral charge collection through the PEDOT:PSS electrode become much more apparent. This can be observed in PEDOT:PSS devices with ~40 nm and ~220 nm films showing an improved fill factor from 39.4% to 60.0% when the sheet resistance was decreased from 2800  $\Omega/\square$  to 160  $\Omega/\square$ . Due to the competing effects of the photocurrent and fill factor, the PCE efficiency of the devices saturates to ~3% as the thickness of the PEDOT:PSS electrode is increased. Solar cells fabricated from ITO-coated glass substrates had an average PCE of ~4.20%,  $J_{sc}$  = 10.25

mA/cm<sup>2</sup>, FF = 66.6% and  $V_{oc}$  = 0.62 V which are over 1% higher than the PEDOT:PSS based electrodes. This is due to the higher transparency (~10% higher) and lower sheet resistance (~10 times less) as compared to the ~220 nm thick PEDOT:PSS electrode.

To demonstrate that this PEDOT:PSS electrode can be applied onto flexible substrates, solar cells using a ~175 nm PEDOT:PSS electrode were fabricated onto plastic substrates. The devices fabricated from the PEDOT:PSS electrode show similar performance (PCE ~3%) to that of solar cells fabricated onto glass substrates as shown in Fig. 5b. These cells are still however ~20% lower in efficiency compared to ITO based plastic substrates which have an average PCE of ~3.7%. Another important consideration for the practicality of flexible electronics which is often ignored is the mechanical stability. The mechanical stability of these flexible solar cell devices was evaluated by subjecting them to a cyclic bending (bend radius ~7.4 mm) test. Fig. 6a shows the illuminated  $J$ - $V$  characteristics of a flexible ITO based electrode device subjected to multiple bending cycles. As the number of bend cycles is increased, a decrease in  $J_{sc}$  and fill factor can be observed and eventually even a lowering of  $V_{oc}$ . This was compared to devices fabricated from the PEDOT:PSS electrodes which show negligible degradation in  $J_{sc}$  and  $V_{oc}$ , but some slight

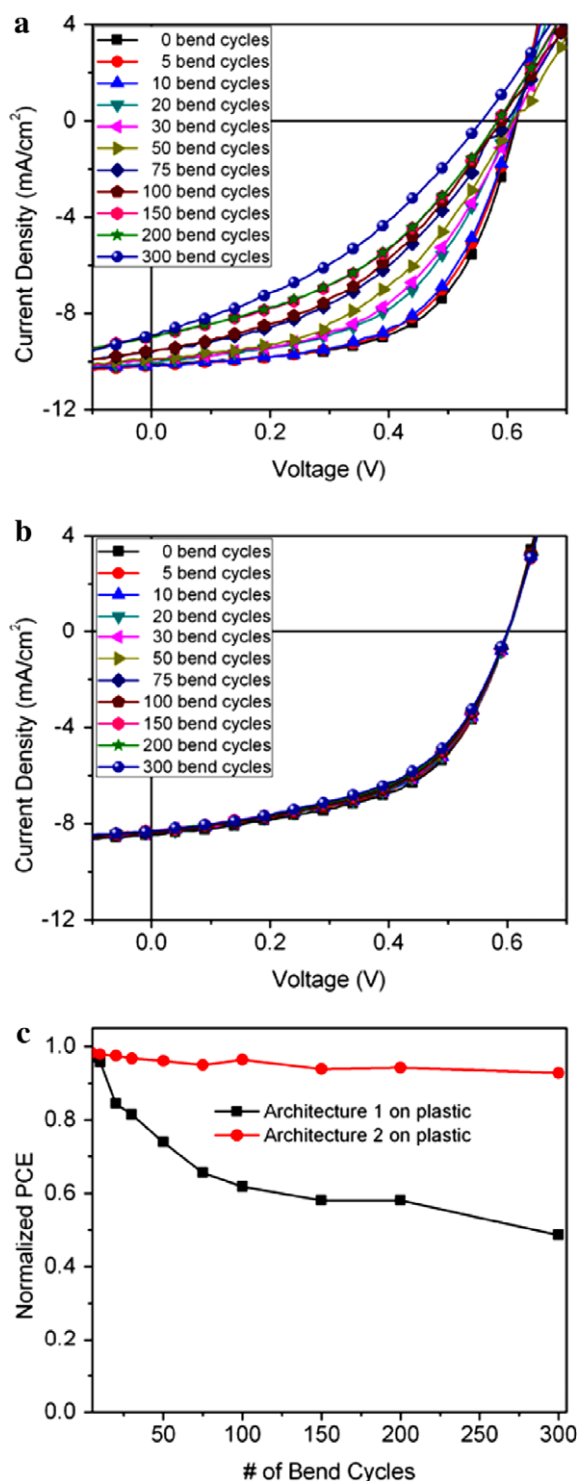


**Fig. 6.** (a) Plot of illuminated  $J$ - $V$  characteristics of inverted devices fabricated from flexible ITO electrode substrates under multiple bending cycles. (b) Plot of illuminated  $J$ - $V$  characteristics of inverted devices fabricated from flexible PEDOT:PSS - 5% DMSO electrode substrates under multiple bending cycles. (c) Comparison of the normalized power conversion efficiency of devices fabricated from flexible ITO and flexible PEDOT:PSS electrodes as a function of bending cycles.

degradation in fill factor after multiple bend cycles (Fig. 6b). The normalized device efficiency of these electrodes were compared as a function of bending cycles showing a retention of  $\sim 92\%$  in the PEDOT:PSS electrodes while only  $\sim 50\%$  in the ITO electrodes after 300 bend cycles (Fig. 6c). The improved mechanical stability from the PEDOT:PSS electrodes as compared to ITO electrodes is an important step to the eventual realization of flexible electronic devices.

Recently, there has been a successful demonstration of spraycoating PEDOT:PSS as an anode electrode in inverted solar cells achieving efficiencies of  $\sim 2\%$ , however, this electrode is thick and non-transparent [22]. We have developed a technique to selectively remove the PEDOT:PSS buffer layer in our inverted solar cell by using a patterned PDMS stamp (Fig. 7). By heating the substrates at an elevated temperature ( $\sim 120^\circ\text{C}$  for 30 s) with the PDMS stamp, the stamp can be removed to selectively lift-off regions of PEDOT:PSS leaving behind the hydrophobic polymer/PCBM active layer. By spincoating solutions of the highly conductive PEDOT:PSS which only wets the PEDOT:PSS buffer layer, a patterned top semi-transparent an-

ode electrode can be formed. From this, semi-transparent inverted devices using ITO-coated glass substrates as the cathode and PEDOT:PSS as the top anode were fabricated. Fig. 5c shows the log  $J$ - $V$  characteristics of these semi-transparent solar cells. These solar cells had an average PCE of 2.51%, a  $V_{oc} = 0.61\text{ V}$ ,  $J_{sc} = 7.86\text{ mA/cm}^2$ , and  $FF = 52.0\%$ . The lower performance especially in photocurrent is most likely due to the non-reflective electrode which unlike Ag does not reflect any unabsorbed light back into the active layer for further absorbance. In addition, the higher sheet resistance of the electrodes (ITO  $15\ \Omega/\square$ , PEDOT:PSS  $\sim 370\ \Omega/\square$ ) can also contribute to losses in device performance. Furthermore, an all solution processed semi-transparent inverted solar cell is demonstrated by replacing the bottom ITO electrode with a PEDOT:PSS electrode. These PEDOT:PSS top anode and PEDOT:PSS bottom cathode solar cells show a PCE of 0.47%,  $V_{oc} = 0.31\text{ V}$ ,  $J_{sc} = 5.49\text{ mA/cm}^2$  and  $FF = 27.7\%$ . The relatively low efficiency is attributed to the much higher sheet resistance of the two electrode contacts ( $>400\ \Omega/\square$ ) which leads a significant deterioration in all the solar cell performance parameters due to the high resistance from the lateral

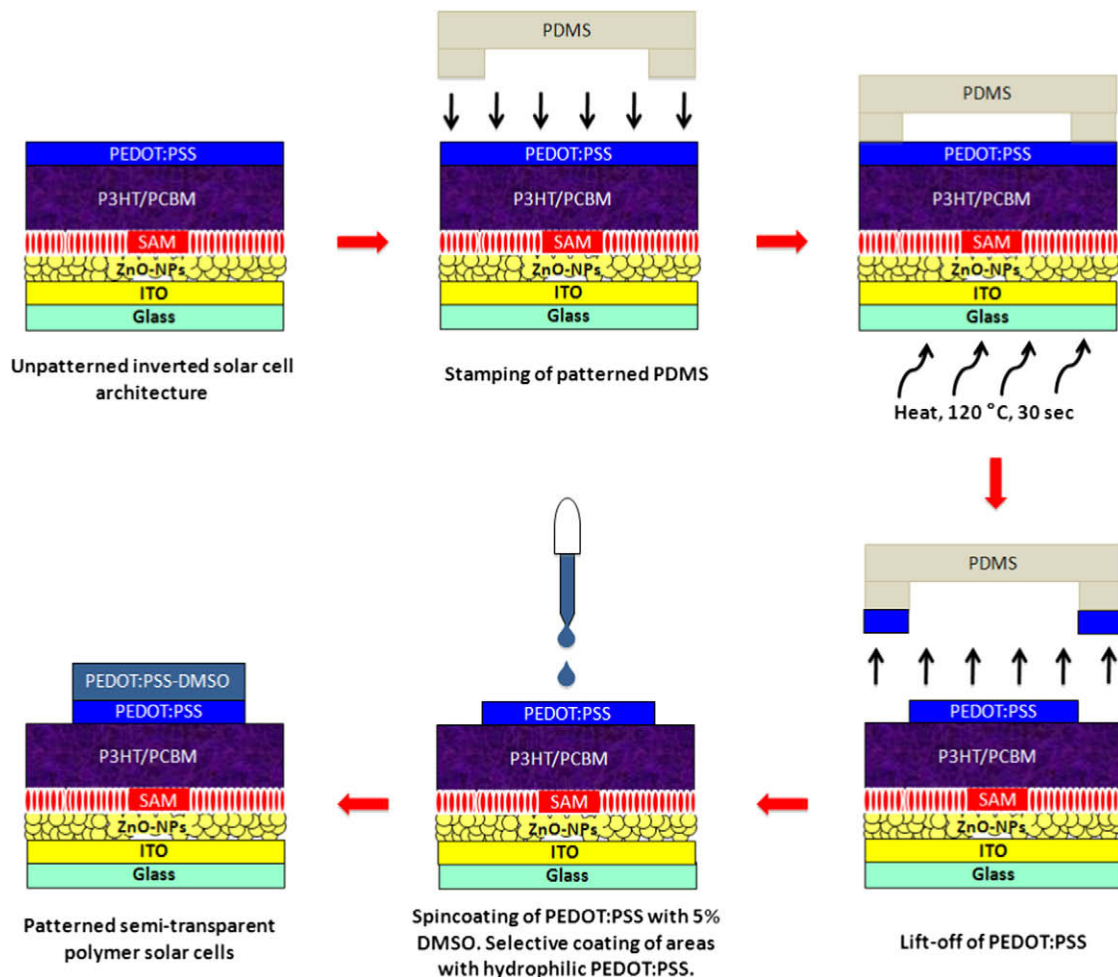


**Fig. 7.** Schematic of patterning PEDOT:PSS by PDMS removal of PEDOT:PSS. Selective removal of the hydrophilic PEDOT:PSS leaves behind the hydrophobic P3HT:PCBM film where spincoating of the conducting PEDOT:PSS–DMSO wets only the region with the PEDOT:PSS pattern leading to semi-transparent solar cells.

charge transport through the PEDOT:PSS electrodes. In addition, the significant drop in  $V_{oc}$  is likely attributed to the reduced built-in field of the device due to the symmetric PEDOT:PSS electrodes used for both contacts. Because of the high sheet resistance, the active device area is limited to a small area in order to minimize the lateral current losses through the electrodes. The sheet resistance of two electrode contacts can potentially be improved by using metalized grids. Using very dense metalized grids should limit the lateral current flow losses and lead to lower sheet resistances. This approach will become important when considering the scaling of the size of the solar cell device to larger active areas.

In conclusion, the replacement of ITO with PEDOT:PSS as the cathode electrode in inverted solar cells has been demonstrated. As the thickness of the PEDOT:PSS electrode was systematically increased, both the transparency and sheet resistance decreased which affected the photocurrent and fill factor of the solar cells. As the transparency of the electrode decreased, the available photons to be absorbed by the active layer were reduced leading to a lower photocurrent density. However, this lowering of photocurrent was offset by an increase in fill factor due to the lower sheet resistance which led to saturation in PCE of  $\sim 3\%$  as the electrode thickness was increased. These PEDOT:PSS electrodes were applied onto flexible plastic substrates showing similar device efficiencies to devices fabricated on glass. The flexible PEDOT:PSS electrodes has better mechanical stability than the flexible ITO based electrodes showing a conversion efficiency retention of  $\sim 92\%$  as compared to  $\sim 50\%$  under 300 cyclic bends, respectively. Semi-transparent inverted solar cells using ITO as the cathode and PEDOT:PSS as the top anode showed PCE of 2.51%. A completely solution processed semi-transparent inverted solar cell was demonstrated by replacing the ITO cathode with a PEDOT:PSS cathode and a PEDOT:PSS top anode showing efficiencies of 0.47%. The semi-transparency of these devices can potentially lead to window based solar applications or other application where semi-transparency is required. More importantly, the replacement of ITO as a transparent electrode with a cheaper transparent electrode will be needed to realizing low-cost flexible polymer solar cells.

## Acknowledgements

This work was supported by the National Science Foundation's NSF-STC program under Project No. DMR-0120967

and the DOE "Future Generation Photovoltaic Devices and Process" program under Project No. DE-FC36-08GO18024/A000. A. K. Y. J. thanks the Boeing-Johnson Foundation for financial support. S. K. H. and H. L. Y. thank the Intel Foundation PhD Fellowship.

## References

- [1] G. Li, V. Shrotryiya, J.S. Huang, Y. Yao, T. Moriarty, K. Emery, Y. Yang, *Nat. Mater.* 4 (2005) 864.
- [2] J. Peet, J.Y. Kim, N.E. Coates, W.L. Ma, D. Moses, A.J. Heeger, G.C. Bazan, *Nat. Mater.* 6 (2007) 497.
- [3] S.I. Na, S.S. Kim, J. Jo, D.Y. Kim, *Adv. Mater.* 20 (2008) 1.
- [4] J. van de Lagemaat, T.M. Barnes, G. Rumbles, S.E. Shaheen, T.J. Coutts, C. Weeks, I. Levitsky, J. Peltola, P. Glatkowski, *Appl. Phys. Lett.* 88 (2006) 233503.
- [5] M.W. Rowell, M.A. Topinka, M.D. McGehee, H.J. Prall, G. Dennler, N.S. Sariciftci, L. Hu, G. Gruner, *Appl. Phys. Lett.* 88 (2006) 233506.
- [6] R.C. Tenent, T.M. Barnes, J.D. Bergenson, A.J. Ferguson, B. To, L.M. Gedvilas, M.J. Heben, J.L. Blackburn, *Adv. Mater.* 21 (2009) 1.
- [7] J. Wu, H.A. Becerril, Z. Bao, Z. Liu, Y. Chen, P. Peumans, *Appl. Phys. Lett.* 92 (2008) 263302.
- [8] V.C. Tung, L.-M. Chen, M.J. Allen, J.K. Wassei, K. Nelson, R.B. Kaner, Y. Yang, *Nano Lett.* 9 (2009) 1949.
- [9] K. Tvingstedt, O. Inganäs, *Adv. Mater.* 19 (2007) 2893.
- [10] M.G. Kang, M.S. Kim, J. Kim, L.J. Guo, *Adv. Mater.* 20 (2008) 1.
- [11] J.Y. Lee, S.T. Connor, Y. Cui, P. Peumans, *Nano Lett.* 8 (2008) 689.
- [12] J. Owen, M.S. Son, K.H. Yoo, *Appl. Phys. Lett.* 90 (2007) 033512.
- [13] J. Hanisch, E. Ahlswede, M. Powalla, *Euro. Phys. J. Appl. Phys.* 37 (2007) 261.
- [14] Y. Zhou, F. Zhang, K. Tvingstedt, S. Barrau, F. Li, W. Tian, O. Inganäs, *Appl. Phys. Lett.* 92 (2008) 233308.
- [15] E. Ahlswede, W. Muhleisen, M. Wahinuddin bin Moh Wahi, J. Hanisch, M. Powalla, *Appl. Phys. Lett.* 92 (2008) 143307.
- [16] J. Ouyang, Q. Xu, C.-W. Chu, Y. Yang, G. Li, J. Shinar, *Polymer* 45 (2004) 8443.
- [17] F. Zhang, M. Johansson, M.R. Andersson, J.C. Hummelen, O. Inganäs, *Adv. Mater.* 14 (2002) 662.
- [18] S. Admassie, F. Zhang, A.G. Manoj, M. Svensson, M.R. Andersson, O. Inganäs, *Solar Energy Mater. Solar Cells* 90 (2006) 133.
- [19] J. Huang, X. Wang, Y. Kim, A.J. deMello, D.D.C. Bradley, J.C. deMello, *Phys. Chem. Chem. Phys.* 8 (2006) 3904.
- [20] S.K. Hau, H.L. Yip, N.S. Baek, J. Zou, K. O'Malley, A.K.Y. Jen, *Appl. Phys. Lett.* 92 (2008) 253301.
- [21] S.K. Hau, H.L. Yip, K. Leong, A.K.Y. Jen, *Org. Electron.* 10 (2009) 719.
- [22] Y.F. Lim, S. Lee, D.J. Herman, M.T. Lloyd, J.E. Anthony, G.G. Malliaras, *Appl. Phys. Lett.* 93 (2008) 193301.
- [23] W.J.E. Beek, M.M. Wienk, M. Kemerink, X. Yang, R.A.J. Janssen, *J. Phys. Chem. B* 109 (2005) 9505.
- [24] S.K. Hau, H.L. Yip, H. Ma, A.K.Y. Jen, *Appl. Phys. Lett.* 93 (2008) 233304.
- [25] S.K. Hau, H.-L. Yip, O. Acton, N.S. Baek, H. Ma, A.K.-Y. Jen, *J. Mater. Chem.* 18 (2008) 5113.
- [26] A. Cravino, P. Schilinsky, C.J. Brabec, *Adv. Funct. Mater.* 17 (2007) 3906.
- [27] M.-S. Kim, M.-G. Kang, L.J. Guo, J. Kim, *Appl. Phys. Lett.* 92 (2008) 133301.
- [28] J. Gilot, M.M. Wienk, R.A.J. Janssen, *Appl. Phys. Lett.* 90 (2007) 143512.